Wide color gamut multi-twist retarders

Kathryn J. Hornburg, Leandra L. Brickson, and Michael J. Escuti

Department of Electrical and Computer Engineering, North Carolina State University, Raleigh, North Carolina 27695, USA

ABSTRACT

We show how highly chromatic Multi-Twist Retarder (MTR) films can be used to create a single-film color filter wherein the color may be selected only by the MTR orientation angle. By this approach, we can create multi-color images with just an MTR between polarizers. We study the design method and limits of the available color gamut possibilities in this approach, and experimentally demonstrate several designs of continuous and discrete patterns. This technique may be useful in art, displays, microscopy, and remote sensing.

Keywords: color filter, waveplate, multi-twist retarder, liquid crystals, imaging, art

1. INTRODUCTION

From the beginning of mankind, humans have been manipulating light and pigments to generate colors representative of the world around them. For example, the increasing knowledge of color theory of pigments shifted humans from using Earth collected materials to synthetic chemical pigments with better color durability and vividness.[1] A similar idea is true with increasing knowledge and technology associated with light manipulation.

In general, the creation of color depends on the mixing and blocking of particular colors outside the wavelengths of interest by controlling the reflectance or transmittance of the film or material. There are several methods to accomplish this mixing task. Color filters generated using differently pigmented transparent medium, like stained glass, dichroic filters, and color gels, can be utilized but must be tiled to reproduce a desired image and unique materials selected for each hue.[2]

Retardation based methods can produce color as well. We can use polarization optics such as one or more homogeneous birefringent plates, such as the Lyot and Šolc family of filters.[3–5] The retarder stacks introduce enhanced blocking of the spectrum outside the wavelength of interest than the individual retarders accomplish by having a variable retardation structure.[6] For the birefringent retarders to work, the thicknesses of each component are tuned so the desired color is output through all the polarizers in the system. The single retarder only works for one specific color and cannot be tuned to work for another without adding or subtracting thickness. Again, like the stained glass, dichroic filter, and gels, these must be tiled and cut to create different color regions within the image. For both stacked and individual retarders, axial rotation only changes the magnitude of its retardation, not its shape or spectral position, therefore different colors cannot be introduced from the rotation of the retarder and additional changes such as temperature or applied voltage will be needed to induce the retardation peak shift desired.[7]

However, this is not an inherent property of all retarders. We describe a complex birefringent film called a multi-twist retarder formed with polymerizeable liquid crystals with markedly different behavior. It manifests a different retardation spectrum for different orientations, because it does not have a true optical axis. Furthermore, this film can create fairly saturated colors in a single physical film, unlike traditional Lyot filter configurations. Furthermore, since this capability can be well controlled with standard processing techniques, it is possible to create full color images within a single birefringent film.

After introducing the relevant background, we will show how this complex retarder can be optimized for a wide color gamut, and study its features and limitations. Finally, we propose and simulate an image based on this approach, where the pixel color is set by the surface orientation on a single substrate.

Correspondence should be sent to: mjescuti@ncsu.edu, Telephone: +1 919 513 7363

Emerging Liquid Crystal Technologies X, edited by Liang-Chy Chien, Harry J. Coles, Hirotsugu Kikuchi, Ivan I. Smalyukh,
Proc. of SPIE Vol. 9384, 93840W · © 2015 SPIE · CCC code: 0277-786X/15/$18 · doi: 10.1117/12.2084853

2. BACKGROUND

2.1 Color Theory

Colors can be represented a variety of different ways. Human vision can be represented as a series of three tristimulus values, imitating the response to the world with the eye's cell structures. These cones give approximately the red, green, and blue response to a scene.[8] We want to mix colors in a way that is closet to what we see to remove more errors within the system. Perceived color is a sum of the response of the three pigments, and color theory allows us to work in more concrete terms by developing color coordinates. However, while a particular radiometric spectrum can be mapped to a unique photopic color coordinate, the inverse is not true - many spectra can lead to the same perceived color. This leads us to the idea of color-mixing. The mixing can be subtractive or additive. The difference between the two systems is binary. The colors combined either provide white (additive, light mixing) or black (subtractive, pigments).[9] In our work, we use chiral doped nematic liquid crystals and assume broadband white visible light, assuring we have an additive system.

To quantify the extent of human vision, a color system that generated a region of all the available colors for humans was developed first by the CIE society in the 1930's called the CIE XYZ color space.[10] Later developments introduced other spaces like La*b* and Lu'v'. All these systems have a specific color matching function so that transfer between systems and between transmission space is possible.[8,10] For color modeling, we select CIE Lu'v' since it has a nearly uniform perceivable color spatial distribution.[8] This means that the perceivable color difference between two different points is independent of their location in CIE Lu'v' space.

2.2 The Multi-Twist Retarder

Multi-Twist Retarders (MTRs) are chiral doped liquid crystal coatings which are applied to a single self-aligning substrate.[11,12] The liquid crystals are aligned initially using Light Polymerizable Polymer (LPP) that is set to an orientation using controlled linearly polarized UV light. By using chiral doped liquid crystals, an additional parameter of twist, ϕ_M, is introduced to the parameters of thickness, d_M, and initial orientation, ϕ_0. In Figure 1(a) we see these parameters on an achromatic MTR. These MTR parameters in series along the axis of light transmission are called the (ϕ, d) vector, shown in the order of $[\phi_0, \phi_1, d_1, ...\phi_M, d_M]$. In total, a set of MTR design parameters gives $2M + 1$ definable elements for the system.

In Figure 1, we illustrate a simple liquid crystal retarder (a) which does not have twist within the layer coated onto the substrate and an achromatic MTR (b) which has twist added to the coated thicknesses. By utilizing color matching functions on the varying transmission of the retarders, rotated from the designed ϕ_0 to $\phi_0 + 90°$ in $1°$ steps between crossed linear polarizers, we look at the apparent color in CIE Lu'v' color space. Let us compare to traditional retarders and an achromatic MTR designed previously by Komanduri.[11] In the color space illustrated in Figure 1 (c), a simple retarder only shows one specific color of green, due to the designated thickness, for all the rotations of the retarder. With the previously designed achromatic MTR, 3TR-A, the output colors in Lu'v' space form a line due to retarder rotation. Previous MTRs for achromatic and chromatic methods utilized constant or wavelength varying target Stokes vectors at the output of the retarder, which gave solutions to the cost functions for only a single angle ϕ_0 the starting orientation.[11,12]

By viewing the result in color space for the achromatic MTR, we get a hint of what will happen if we establish target profile primaries similar to those in human eyes. Instead of keeping the initial orientation constant while fitting each target profile, we see what will happen if the orientation angle is changed and the other (ϕ, d) parameters are held constant. The goal with this is to define a wide gamut that allows easy color reconstitution by covering many colors.

3. DESIGN PROCESS

The design process associated with wide gamut MTRs is multi-faceted. To have a good design, a gamut has to be developed that covers as much of the available color space as possible, plus has a set of colors in the gamut that correspond back to a target image correctly. This includes the step of accurately mapping colors outside of the gamut to the gamut with minimal loss of color information.

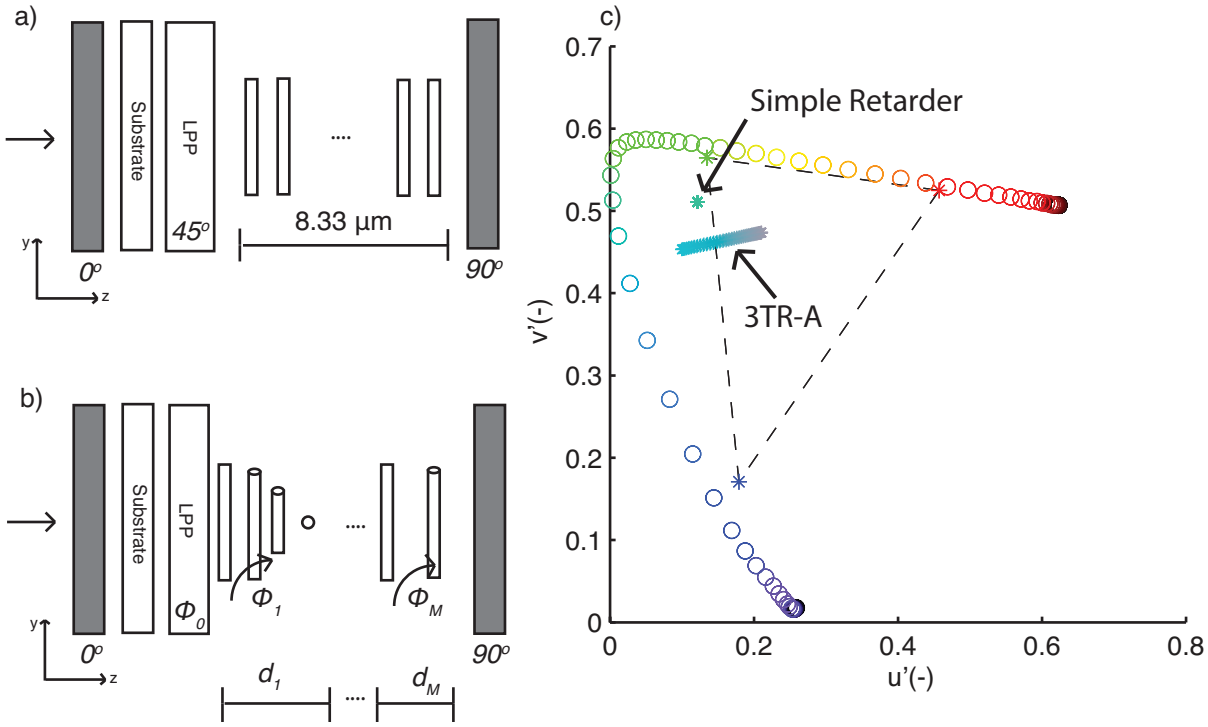

Figure 1. Two different forms of liquid crystal retarders a) a simple retarder for green light and (b) an achromatic MTR. In (c) we rotate both retarders and compare the apparent colors at the output of the retarders. The dashed triangle with colored star corners indicates the range of RGB colors available with Matlab, the modeling software utilized for this work.

3.1 MTR Design for a Wide Color Gamut

The process of creating and designing a MTR begins with modeling each layer as a twisted nematic cell and using the birefringence profile for the chosen base liquid crystal mixture. In this study, we used RMS03-001c (Merck Chemicals, Inc.) with a birefringence profile of $\Delta n = 0.128 + 8340/\lambda^2$ and assumed the low doping needed to induce the twist term, less than 1% of volume of the main liquid crystal, would not change the birefrigence profile from that given for RMS03-001c. This handling is the same as achromatic and chromatic MTRs.[11,12] The major difference for wide gamut MTRs is the parsing of the (ϕ, d) vector. The development of wide gamut MTRs is associated with the ability to use multiple orientation directions that can lead to a variety of colors. For this, we needed to develop a new handling system for this subset of MTRs. In Table 1, we illustrate the MTR design matrix for wide gamut MTRs. To relate back to traditional display technology, we provide orientation angles that result in the best red, green, and blue colors, although many other primaries outside of this range can be selected to provide better color mixing.

Table 1. The format of the MTR parameters used in this work.

ϕ_0 Green	Twist Layer 1	Thickness Layer 1	... ...	Twist Layer M	Thickness Layer M	ϕ_0 Red	ϕ_0 Blue
$\phi_{0,G}$	ϕ_1	d_1	...	ϕ_M	d_M	$\phi_{0,R}$	$\phi_{0,B}$

Unlike the previous methods of achromatic and chromatic, wide gamut MTRs require a target function that is not achromatic, and instead varies with wavelength in a similar manner to the tristimulus values. Also, we keep in mind the expected results from our MTR elements, and maintain a profile that is similar to the MTR

element's expected results, not a perfect step function for each region. We choose Gaussian-stylized functions with sharp cutoffs outside the specific color band through crossed linear polarizers, similar to the color matching functions utilized with CIE systems.[8,10] Previously, Stokes vectors of the target output, $\mathbf{S^t}$, have been used to represent the target functionality of the MTR. This is continued with the wide gamut work with more target profiles used to correspond to each tristimulus value. With this work, the target functions take on the following form, where the wavelength dependence can be thought of as the third dimension of the multidimensional matrix:

$$\mathbf{S^t}(\lambda) = \begin{bmatrix} 1 & 1 & 1 \\ R(\lambda) & G(\lambda) & B(\lambda) \\ 0 & 0 & 0 \\ 0 & 0 & 0 \end{bmatrix} \tag{1}$$

Where we have R, G, B correspond to the red green and blue wavelengths which have different values depending on which tristimulus value is being investigated.

To relate these directly to the tristimulus values we would have as follows:

$$\mathbf{S^t_R}(\lambda) = \begin{bmatrix} 1 & 1 & 1 \\ -g(\lambda, \overline{R}, \sigma_R) & 1 & 1 \\ 0 & 0 & 0 \\ 0 & 0 & 0 \end{bmatrix} \tag{2}$$

$$\mathbf{S^t_G}(\lambda) = \begin{bmatrix} 1 & 1 & 1 \\ 1 & -g(\lambda, \overline{G}, \sigma_G) & 1 \\ 0 & 0 & 0 \\ 0 & 0 & 0 \end{bmatrix} \tag{3}$$

$$\mathbf{S^t_B}(\lambda) = \begin{bmatrix} 1 & 1 & 1 \\ 1 & 1 & -g(\lambda, \overline{B}, \sigma_B) \\ 0 & 0 & 0 \\ 0 & 0 & 0t \end{bmatrix} \tag{4}$$

With g representing a Gaussian-styled function at a certain wavelength, λ, which has a mean in red, R, green, G, or blue, B, as specified as the target function for the tristimulus value. The standard deviation of the Gaussian function is σ, where $\sigma = FWHM/\sqrt{2ln(2)}$ with FWHM as the size of the wavelength band in the color. To solve the target profile and compare different (ϕ, d) vectors to each other, a cost function, f, is utilized. The cost function can be chosen differently depending on the result that is desired to be maximized. The major cost function form used for this paper was:

$$f = rms(\mathbf{T_{\perp R}}(\lambda) - \mathbf{T^t_{\perp R}}(\lambda)) + rms(\mathbf{T_{\perp G}}(\lambda) - \mathbf{T^t_{\perp G}}(\lambda)) + rms(\mathbf{T_{\perp B}}(\lambda) - \mathbf{T^t_{\perp B}}(\lambda)) - 2(FracArea/100) \tag{5}$$

We can relate the $\mathbf{S^t_{RGB}}(\lambda)$, the target Stokes vector at the output of the retarder for red, green,and blue output colors, to $\mathbf{T^t_{\perp RGB}}(\lambda)$, the target transmission through crossed linear polarizers for red, green, and blue output colors by:

$$\mathbf{T^t_{\perp RGB}}(\lambda) = (1 - \mathbf{S^t_{1,RGB}}(\lambda))/2. \tag{6}$$

In Figure 2, both the $\mathbf{S^t_{RGB}}(\lambda)$ and $\mathbf{T^t_{\perp RGB}}(\lambda)$ target profiles are shown. In actuality, these Stokes vectors at the output of the retarder are modulating the $\mathbf{M_{1..2,1..2}}(\phi_0, \lambda)$, the upper left corner of the Mueller matrix where the retarder is described as a function of orientation and wavelength.[3] In CIE Lu'v' space, the $\mathbf{T^t_\perp}$ corresponds to [0.29, 0.55, 0.52] as red , [0.78, 0.05, 0.58] as green, and [0.025, 0.20, 0.08] as blue.

The fractional area, $FracArea$, utilized in f is a comparison of the area coverage of the u'v' space by different gamuts with no regard to the luminance. This converts the 2-D representation of u'v' space commonly used to 1-D by giving the one coordinate value of area. Using this gives another weighting value that can be put within the cost function. As an example, the RGB space as defined by Matlab is 32% of the total CIE Lu'v' color space.

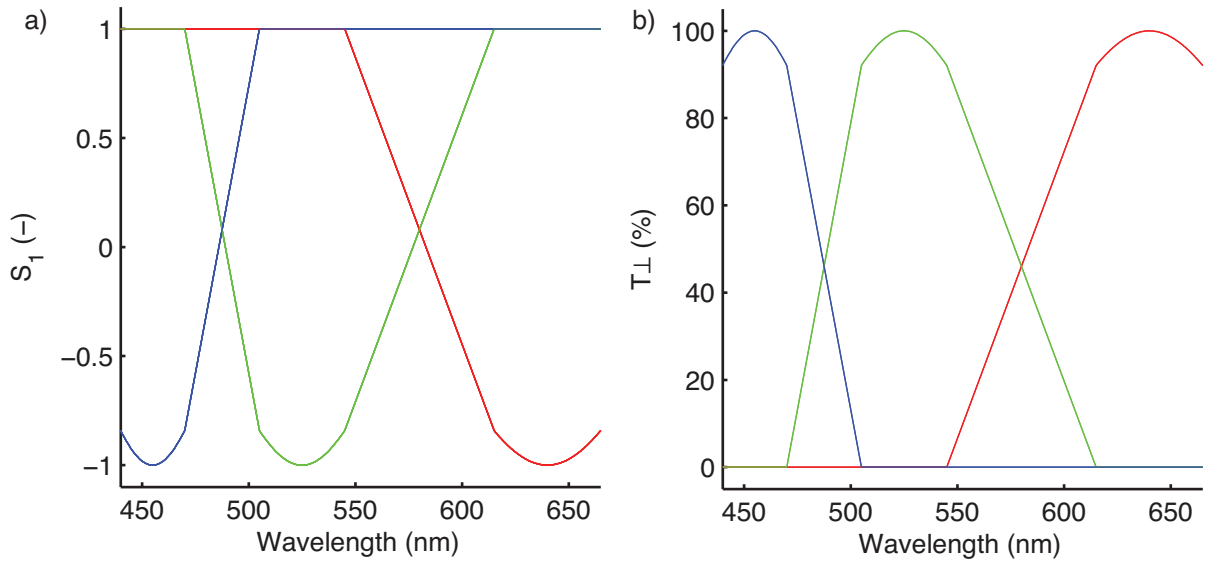

Figure 2. Target profiles utilized for creating MTR designs (a) shows the modulation of the $\mathbf{S_1}$ for multiple wavelengths in RGB and (b) illustrates the same change just as a transmission through crossed linear polarizers.

3.2 Image Reconstruction

One example of an application of wide color gamut MTRs would be the realization of a full color image, observable by viewing the MTR through crossed polarizers. In order to convert any image into a colored MTR, the image's color span must be adjusted to be only colors within the gamut of the MTR. Therefore, each pixel of the image needs to be reconstructed using the MTR gamut. These pixels will then be represented as a combination of ϕ_0 values, as shown in Figure 3.

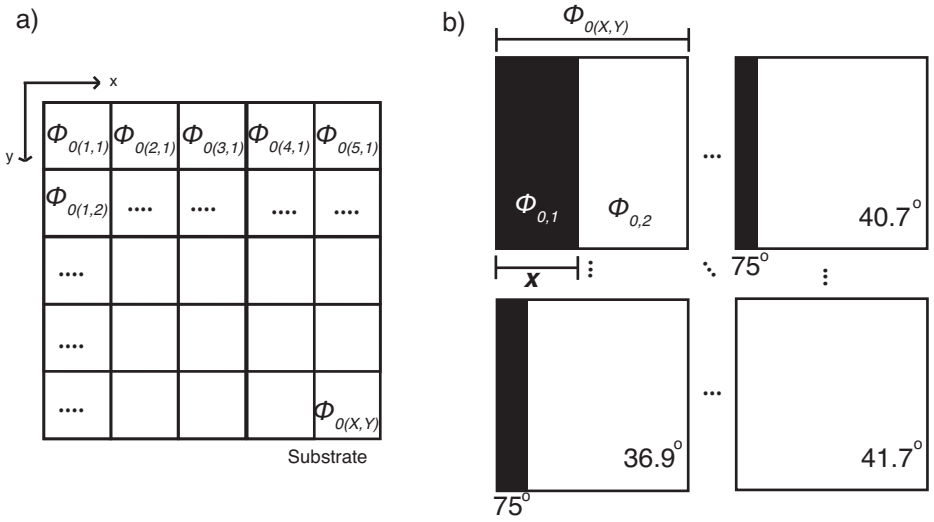

Figure 3. (a) Orientation angle, ϕ_0, that is changed across the substrate for each pixel, according to the test image's coloring scheme. (b) The pixel arrangement of 4 different pixels enclosed in the test image.

There are two cases to deal with in the color regeneration: inside and outside the gamut. If the desired color is outside the gamut, it is mapped to the nearest point on the border of the gamut, and will be made by a

pixel entirely of that orientation. This is shown in Figure 4 (a). We predict some color distortion through this approximation, however for colors outside the gamut, this is the best that the MTR can realize.

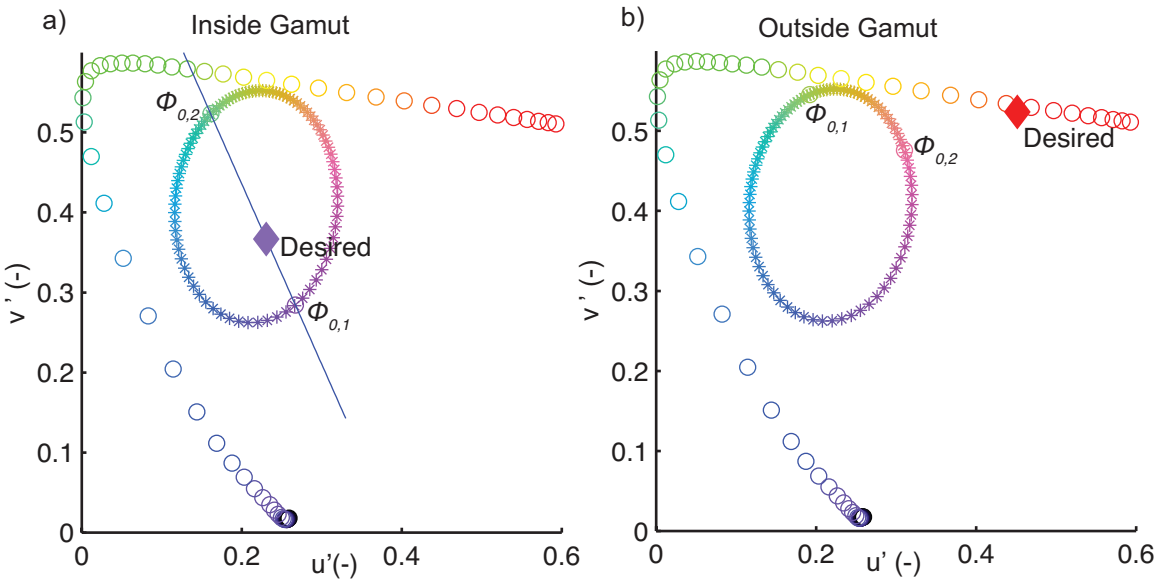

Figure 4. There are two cases for solving $\phi_{0,1}$, $\phi_{0,2}$, and $\mathbf{X}$ for a desired color. For a color within the gamut (a), we solve for $\phi_{0,2}$ given a desired color within the gamut and starting $\phi_{0,1}$ by generating a line between the desired color and $\phi_{0,1}$.We reduce distance of $\phi_{0,2}$ to that line using a minimization process. For colors outside the gamut (b),$\phi_{0,2}$ is found closest to the desired color. In this case, $\phi_{0,1}$ and $\mathbf{X}$ are not used for color reconstruction.

If the color is inside the gamut, a combination of colors will be needed. Using two orientation angles, each corresponding to a color on the border of the gamut, a line can be drawn between the two points to visualize what colors are possible when combining them. By controlling the relative intensities of the two angles, any color along the line can be made.This is shown in Figure 4 (a).

Typically in color mixing, combinations of two colors are controlled by adjusting the intensity of each primary. This intensity ratio determines where along the line between them the resulting color will be.[10] However, in MTR application, the transmission intensity of a certain orientation angle is not adjustable. Therefore, for this research the relative intensity is adjusted by controlling the relative area each orientation angle occupies within the pixel. This is shown in Figure 3 (b). Using this method, we are able to realize any color within the gamut. The process used to solve for the angles and relative area needed to best represent any color for a given gamut defined by the MTR is detailed in the remainder of this section. In this work, the term 'relative area' refers to how the pixel is made and is defined as:

$$\mathbf{A_R} = A_{\theta 1}/A_{\theta 2} \tag{7}$$

$A_{\theta 1}$ and $A_{\theta 2}$ are the areas occupied by $\phi_{0,1}$ and $\phi_{0,2}$, respectively, within the pixel. This related to the pixel as a parameter $\mathbf{X}$ shown in Figure 3 (b), and is defined by:

$$\mathbf{X} = A_R/(1 - A_R) \tag{8}$$

To reconstruct a pixel, we begin with a desired color and (ϕ, d) vector. The desired color is then converted to u'v' space and plotted on the gamut. For this study, a $\phi_{0,1}$ is arbitrarily chosen and a $\phi_{0,2}$ is solved. The solution of $\phi_{0,2}$ occurs when a line drawn between Angle1 and Angle2 intercepts the desired color on the uv plane. This is done by an iterative minimization fit. The angle found for $\phi_{0,2}$ using this method is the best fit for any color inside the gamut. From $\phi_{0,1}$, $\phi_{0,2}$, and the desired color, we can use a simple comparison to see if we are within the gamut. If the u'v' distance from desired color to either $\phi_{0,1}$ or $\phi_{0,2}$ is larger than the distance between $\phi_{0,1}$ and $\phi_{0,2}$, we are outside the gamut. Otherwise we are within the gamut and our calculation for $\phi_{0,1}$ and $\phi_{0,2}$ is correct. We find the relative area between the angles as the ratio of lengths:

$$\mathbf{A_R} = Distance_{\phi_{0,2}toDesired}/Distance_{\phi_{0,1}to\phi_{0,2}} \tag{9}$$

If we find the color to be outside the gamut, an additional iterative minimizer needs to be done to find the nearest color on the border of the gamut. A $\phi_{0,2}$ is solved using iteration to minimize the distance from $\phi_{0,2}$ and the desired color. Our pixel will consist of only the $\phi_{0,2}$ and the relative area will be 0.

4. RESULTS

Utilizing the cost function specified during development, a 3TR MTR was found that has a sizable region of the Lu'v' color space enclosed. The (ϕ, d) vector is given in Table 2. This 3TR has a fractional area of 24%. The best primaries for red, green, and blue are located at [0.36, 0.51, 0.30], [0.46, 0.16, 0.53] and [0.13, 0.17, 0.28] respectively. This is indicated by the three black circles in Figure 5 (a) and the three black stars in Figure 5 (b).

Table 2. (ϕ, d) vector of 3TR MTR selected for development.

$\phi_{0,G}(^\circ)$	$\phi_1(^\circ)$	$d_1(\mu m)$	$\phi_2(^\circ)$	$d_2(\mu m)$	$\phi_3(^\circ)$	$d_3(\mu m)$	$\phi_{0,R}(^\circ)$	$\phi_{0,B}(^\circ)$
-8.1	-60.9	1.41	11.1	3.02	64.4	1.38	40.2	-68.7

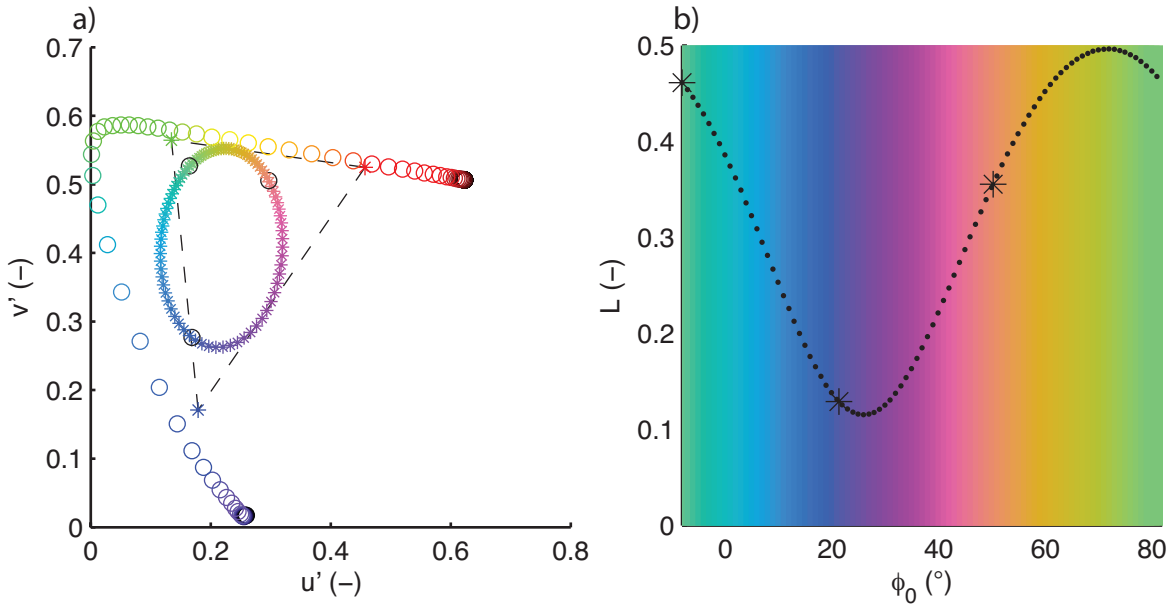

Figure 5. The modeled (ϕ, d) region where (a) shows the u'v' gamut with an overlayed RGB triangle gamut illustrating the limitations of the simulation software in showing varying colors while (b) gives the third dimension L. The black stars in (b) match to the orientation angles of the best primaries for red, green, and blue shown by black circles in (a).

To test image reconstruction, three test images were selected to test a variety of colors and luminances. These three images are shown in Figures 6 (a), 7 (a) and 8 (a). These were reconstructed using the color matching process from development and the resulting images are shown in Figures 6 (b), 7 (b) and 8 (b). Figures 6 (c), 7 (c) and 8 (c) show all color points in u'v' space that were used to reconstruct the image. The images were simulated using the MTR detailed in Table 2 and a $\phi_{0,1}$ of 75°.

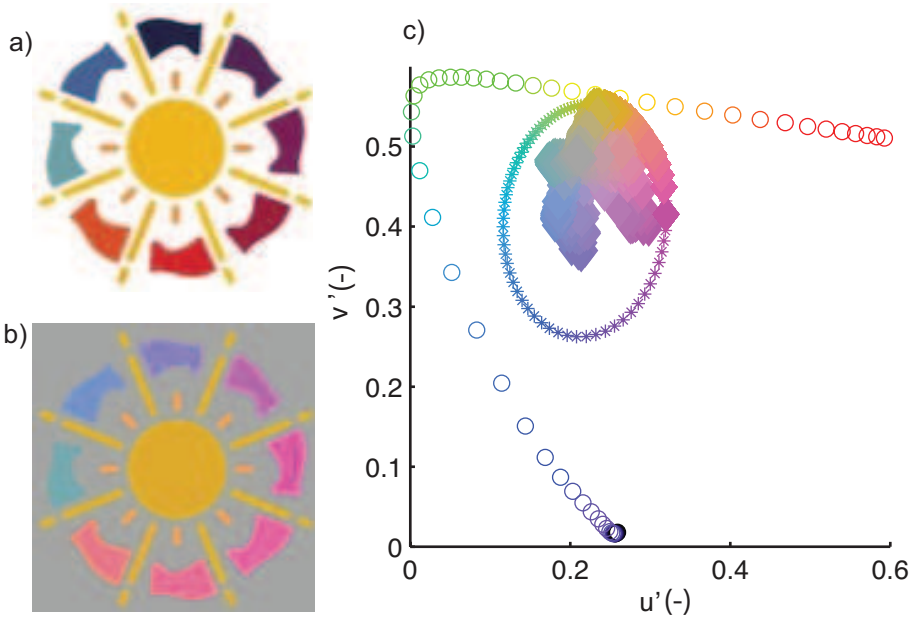

Figure 6. The original International Year of Light (IYL) 2015 logo (a) and reconstructed International Year of Light (IYL) 2015 logo (b) image using the MTR detailed in Table 2. (c) Color map illustrating the color points used to reconstruct the image.

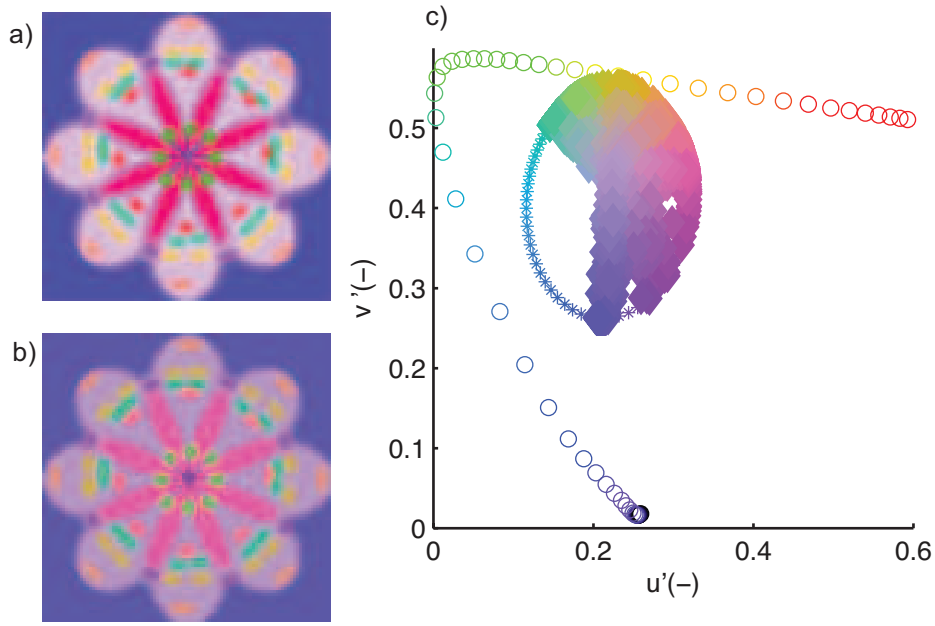

Figure 7. The original flower image (a) and reconstructed flower image (b) using the MTR detailed in Table 2. (c) Color map illustrating the color points used to reconstruct the image.

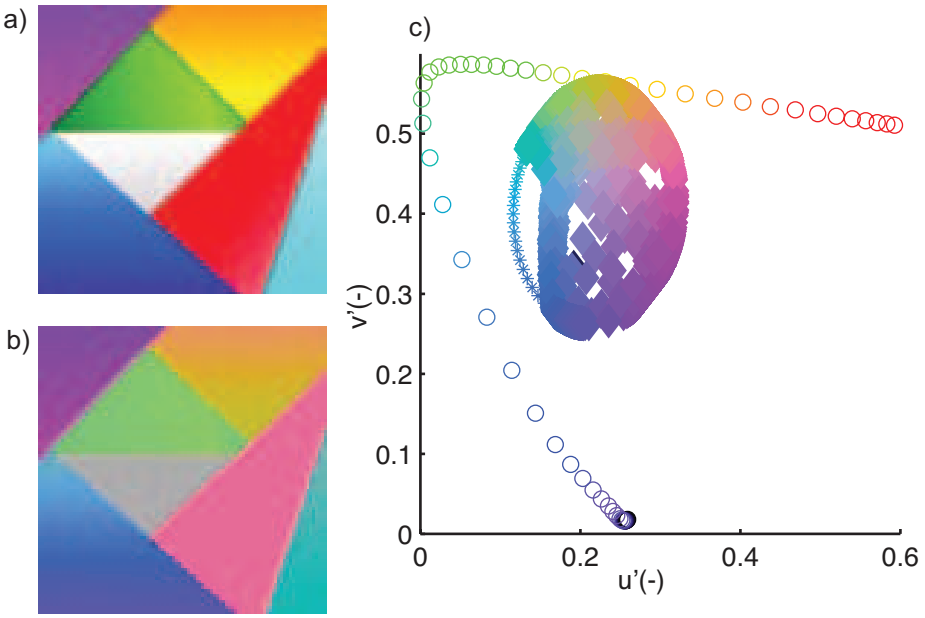

Figure 8. The original triangle image (a) and reconstructed triangle image (b) using the MTR detailed in Table 2. (c) Color map illustrating the color points used to reconstruct the image.

5. DISCUSSION

The best primaries associated with the red, green, and blue orientation angles give distance errors of 0.27, 0.35, and 0.23 respectively. This is due to the luminance for green not reaching the same level as the target point and both the u'v' value for red and blue not reaching their respective targets. Our original target specified 63% CIE

Lu'v' total area. The application of the 3TR MTR results in 39% drop in area from the target specification. We are now working to experimentally realize the MTR design proposed and simulated here.

During image reconstruction using a wide gamut MTR, we observed that colors within the gamut lead to a color of the same u' and v' values, but a different L. This leads to a change in luminance in the reconstructed pixel, causing a slight alteration from the desired color's brightness. Because of this, very bright or dark regions suffer the most during image reconstruction. As we can see from the reconstructed images in Figures 6 (b), 7 (b) and 8 (b), the large color range displayed by the MTR's gamut allows us to represent most of the image's color without significant distortion. As predicted, we can see that the largest color alterations occur when the desired color lies outside of the gamut, or when the gamut doesn't allow for the target color's luminance. This is especially apparent in the target colors. Some examples would be white, which shifts to gray; black,which shifts to blues and purples; and red, which shifts to pink. In future work, adding a second MTR film to the system could provide better luminance control of each pixel, giving a wider range in luminance available for image reconstruction.

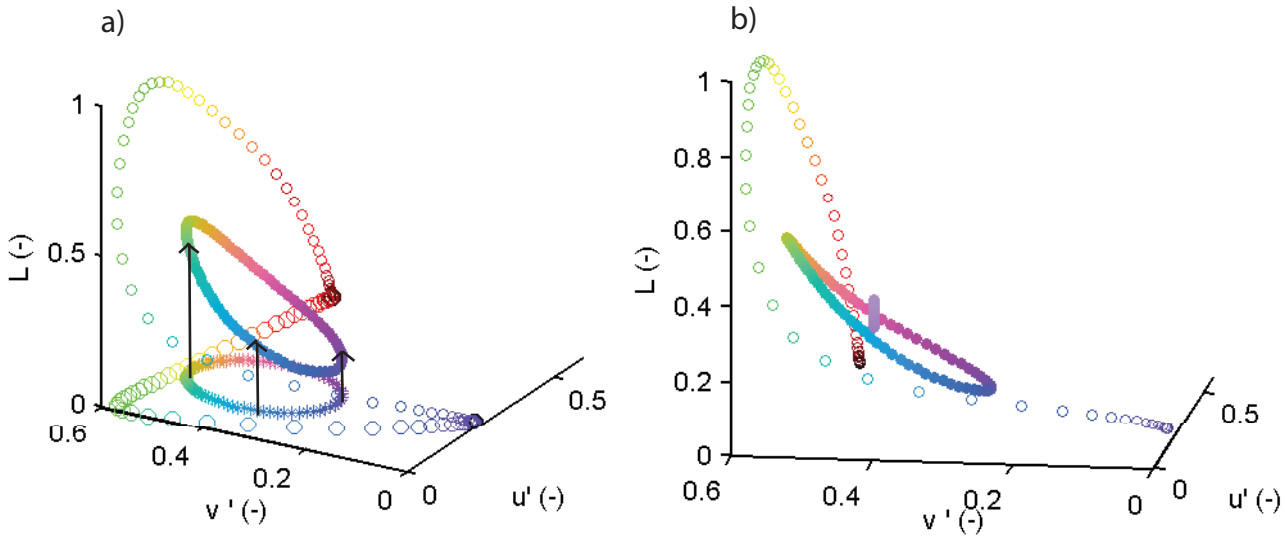

Figure 9. (a) A 3D representation of the gamut is shown projected above the 2D u'v' space gamut, from this we can see the hyperbolic paraboloid characteristics of the gamut. (b) The L parameter varies with changes in $\phi_{0,1}$ values for the same target color.

Figure 9 (a) shows a 3D plot of the gamut displayed over the 2D projection. As we can see, the gamut lies along a curved 3D plane resembling a hyperbolic paraboloid. When colors are constructed on this paraboloid using a combination of two angles, we can draw a line between the two angles selected to find the color that will be realized, as was done in the 2D case. However, since the gamut exists as a 3D curve, rather than a 2D plane, selecting different angles to create the same color will result in slightly different luminance. This is illustrated in Figure 9 (b), which solves for the same RGB point with varying $\phi_{0,1}$. The different $\phi_{0,1}$ lead to a different luminances of the reconstructed color, giving a 7.6% luminance variation in that specific color. This means that although we are not able to control the intensity of the orientation angle's color, we still have some freedom to control the luminance of colors made from the combinations of angles due to the gamut's 3D nature in Lu'v' space. For the reconstruction algorithm used in this work, this could be utilized by finding the best $\phi_{0,1}$ for each pixel.

6. CONCLUSION

We have shown that multi-twist retarders can produce a wide variety of colors within a single film larger than that of individual simple retarders. We have shown a development technique designed to create wide gamut

MTRs. The range of color generated from these MTRs can be used with patterning technology to write and reproduce images using liquid crystals. In simulation, we have shown that MTRs can be used to recolor art by recoloring three images with the 3TR MTR selected in the results section. The images selected were the logo of the International Year of Light (IYL) 2015, a flower, and a set of colored triangles. While some reds, green, blue, and lighter components of the grayscale are well produced; it remains the subject of future work to develop the technique for the creation of black, well controlled grayscale, and saturated reds.

ACKNOWLEDGMENTS

The authors gratefully acknowledge the financial support of ImagineOptix Corporation, within which M.J.E. holds an equity interest. The authors also acknowledge Dr. Ravi Komanduri for helpful discussions.

REFERENCES

[1] Bleicher, S., [*Contemporary Color: Theory and Use*], Thomson Delmar Learning, New York (2005).
[2] Hecht, E., [*Optics*], Addison Wesley, San Francisco, 4th ed. (2002).
[3] Goldstein, D. H., [*Polarized Light*], CRC Press, New York, 3rd ed. (2011).
[4] Šolc, I., "Birefringent chain filters," *J. Opt. Soc. Am.* **55**(6), 621–625 (1965).
[5] Evans, J. W., "A birefringent monochromator for isolating high orders in grating spectra," *Appl. Opt.* **2**(2), 193–197 (1963).
[6] Woltman, S. J., Jay, G. D., and Crawford, G. P., [*Liquid Crystals: Frontiers of Biomedical Applications*], World Scientific, Danvers, MA (2007).
[7] Xia, X., Stockley, J. E., Ewing, T. K., and Serati, S. A., "Advances in polarization based liquid crystal optical filters," *Proc. SPIE* **4658**, 51–58 (2002).
[8] Hunt, R., [*Measuring Colour*], Ellis Horwood, London, 2nd ed. (1991).
[9] Gerritsen, F., [*Theory and Practice of Color*], Van Nostrand Reinhold Company, New York, 2nd ed. (1983).
[10] Trussell, H. and Vrhel, M. J., [*Fundamentals of Digital Imaging*], Cambridge University Press, New York (2008).
[11] Komanduri, R. K., Lawler, K. F., and Escuti, M. J., "Multi-twist retarders: broadband retardation control using self-aligning reactive liquid crystal layers," *Optics Express* **21**, 404–410 (2013).
[12] Hornburg, K. J., Komanduri, R. K., and Escuti, M. J., "Multiband retardation control using multi-twist retarders," in [*Polarization: Measurement, Analysis, and Remote Sensing XI*], Chenault, D. B. and Goldstein, D. H., eds., *Proc. SPIE* **9099**, 90990Z (2014).